Ingeniería y Universidad
ISSN: 0123-2126
ISSN: 2011-2769
Pontificia Universidad Javeriana

Durán-Giraldo, Diego Andrés; González-Sierra,
Carlos Santiago; Merchán-Rincón, Fabio Alejandro

Preliminary Design of the Landing Gear for a CESTOL Aircraft FAR 23*

Ingeniería y Universidad, vol. 26, 2022, January-December, pp. 1-27
Pontificia Universidad Javeriana

DOI: https://doi.org/10.11144/Javeriana.iued26.pdlg

Preliminary Design of the Landing Gear for a CESTOL Aircraft FAR 23[a]

Diseño preliminar del tren de aterrizaje para una aeronave tipo CESTOL FAR 23

Received: July 16, 2020 | Accepted: June 16, 2021 | Published: July 29, 2022

Diego Andrés Durán-Giraldo*
Universidad de San Buenaventura, Bogotá, Colombia
ORCID: https://orcid.org/0000-0001-5467-2978

Carlos Santiago González-Sierra
Universidad de San Buenaventura, Bogotá, Colombia
ORCID: https://orcid.org/0000-0003-0836-0265

Fabio Alejandro Merchán-Rincón
Universidad de San Buenaventura, Bogotá, Colombia
ORCID: https://orcid.org/0000-0002-3401-3913

[a] Research paper - Article of scientific and technological investigation

* Corresponding author. E-mail: daduran@academia.usbbog.edu.co

DOI: https://doi.org/10.11144/javeriana.iued26.pdlg

How to cite this article:
D.A. Durán, C. S. González- Sierra, F. A. Merchán-Rincón, "Preliminary Design of the Landing Gear for a CESTOL Aircraft FAR 23" Ing. Univ. vol. 26, 2022. https://doi.org/10.11144/javeriana.iued26.pdlg

Abstract

Objective: Design the landing gear for a CESTOL type aircraft according to FAR 23 using: (i) the conceptual designs of the nose and main gear and (ii) evaluate the structural strength of the design by means of finite element analysis at a stage of landing. ***Materials and methods:*** The initial requirements for the theoretical development of a preliminary landing gear design are used as a case study. The aircraft's structure is taken as a base for the different design stages. This analysis is according to a static and level landing condition selected on each gear with a side and supplementary load. Additionally, calculations of geometric parameters and mechanical resistance with preselecting materials for the component analysis to determine and compare theoretical results with finite elements to evaluate the reliability of the design approach. ***Results and discussion:*** It is determined to move the main landing gear backward near the cargo area. That allows for better aircraft performance, placing the GC in front of the main gear and avoiding an overturn. However, this load percentage changes in proportion to the longitudinal stability criterion, where it generates an increase in the contribution to the mechanical stress in the structure of the gear. ***Conclusions:*** Results obtained about stability, controllability, and structural analysis are acceptable for the regulations of FAA Part 23 with standards associated with airworthiness, being corroborated with theoretical analysis and combined loads.

Keywords: landing gear, lug, design, materials resistance, finites element.

Resumen

Objetivo: diseñar el tren de aterrizaje para una aeronave CESTOL según FAR 23, mediante: (i) los diseños conceptuales del tren de nariz y tren principal y (ii) evaluar la resistencia estructural del diseño por medio del análisis de elementos finitos en una determinada etapa del aterrizaje***. Materiales y métodos:*** se emplea como caso de estudio los requerimientos iniciales para el desarrollo teórico de un diseño preliminar del tren de aterrizaje, donde la estructura de dicha aeronave se tiene como base para las diferentes etapas de diseño. Este análisis se realiza acorde a una condición de aterrizaje estática y nivelada seleccionada en cada tren con una carga lateral y suplementaria. Adicionalmente, cálculos de parámetros geométricos y resistencia mecánica con materiales preseleccionados para el análisis de componentes con el fin de determinar y comparar los resultados teóricos con elementos finitos para evaluar la fiabilidad del planteamiento del diseño. ***Resultados y discusión:*** Se determina mover el tren de aterrizaje principal hacia atrás cerca de la zona de carga, permitiendo un mejor rendimiento de la aeronave, colocando el CG en frente del tren principal, evitando un volcamiento. Sin embargo, el porcentaje de carga cambia en proporción al criterio de estabilidad longitudinal, generando un incremento de la contribución al esfuerzo mecánico en la estructura del tren. ***Conclusiones:*** los resultados obtenidos en referencia a estabilidad, controlabilidad y análisis estructural son aceptables para la regulación de la FAA Parte 23 con estándares asociados a la aeronavegabilidad, estando corroborado con la teoría analítica y las cargas combinadas.

Palabras clave: Tren de aterrizaje, lug, diseño, resistencia de materiales, elementos finitos

Introduction

The aeronautical development taking place in Colombia has been growing in recent years. Such growth in the Colombian aviation industry is based on the constant passenger increase and cargo transported with an annual growth rate of 9.6% due to a long work that has been developed in the last decade. This led to the generation of new jobs and projects through the development of policies that carried through the growth of the sector in the following years [1]. According to this, the University of San Buenaventura-Bogota decided to design a multipurpose aircraft for the CESTOL category that has applications for the defense sector. This design of the aircraft's structure allows the design of the retractable landing gear for the nose and main landing gear as a structural support and displacement system. The design considers the maximum operating weight and versatility in-ground for each landing gear, as well as the location and form of fastening.

The project has the main objective to develop the design for the landing gear that achieves requirements for its viability and regulatory standards of the authorities in operation, such as FAR 23. Therefore, this document describes the development and structural analysis of the landing gear design for a CESTOL aircraft using the 3D modeling product in the CATIA V5 software. The 3D design is the base for theoretical analysis of the gear in the selected stages and geometric parameters of lateral and longitudinal stability by the aerodynamic and inertial load in the aircraft. Stress calculations such as Finite Element Analysis estimate the safety factors for the loads present in sideload condition on the main gear and the nose gear in the supplementary landing condition. The study methodology has the finality to compare the results obtained by computational analysis with the theoretical results obtaining low error percentages.

Materials and methods

The methodology used for the development of this design is proposed by Mohammad H. Sadraey [2] for the preliminary design of the landing gear in aircraft. On the other hand, the methodology has been done according to the flowchart described in Figure 1, presenting processes used to create design and technical concepts. All of this methodology can be found in the reference [3].

Design requirements

The requirements of the design for landing gear, together with the basic configuration for the aircraft, must have the next two minimum conditions:

- Retractable landing gear for unprepared runways.
- Maximum takeoff weight (MTOW) of 19000lb.

Figure 1. Development flow chart

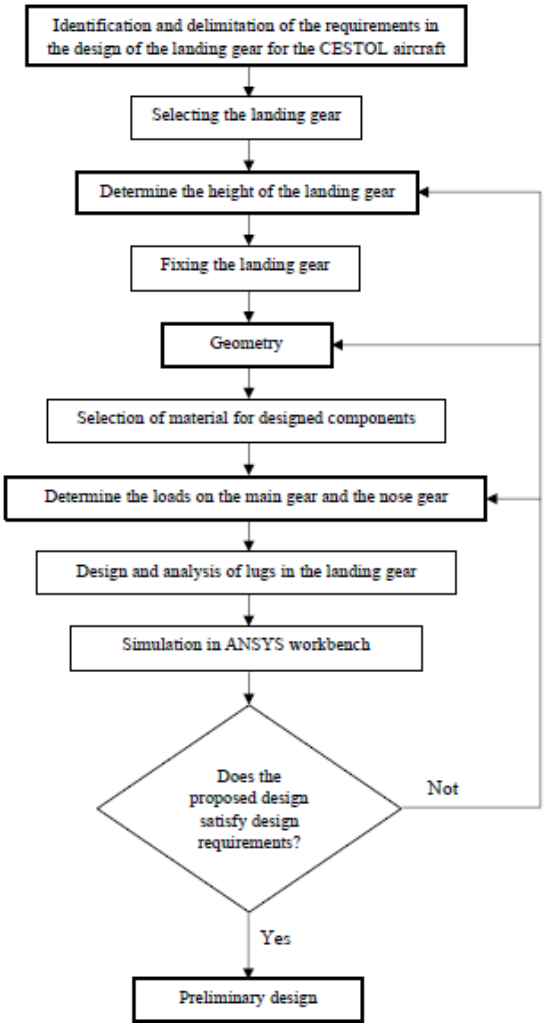

Source: Own source

Aeronautic Normative of FAA

The preliminary design of the landing gear considered the different appendices of FAR 23, 2020 publication. References to the loads that the landing gear must resist in landing stages established and some parameters of configuration [4], as follows:

FAR 23.2155 Ground and water handling characteristics: For airplanes destined for operation on land or water, the airplane must have controllable longitudinal and directional handling during taxiing, takeoff, and landing operations.

FAR 23.2220 Ground and water load condition: The applicant must determine the structural design loads resulting from taxiing, takeoff, landing, and handling condition on the applicable surface in normal and adverse attitudes and configurations.

FAR 23.2265 Special factor of safety:

(a) The applicant must determine a particular safety factor for each critical design value for each part, item, or assembly. That critical design value is uncertain for each part, item, or assembly.
(b) The applicant must determine a special factor of safety using quality controls and specifications that account for each.
(c) The applicant must multiply the highest pertinent special factor of safety in the design for each part of the structure by each limit and ultimate load or ultimate load only if there is no corresponding limit load, such as emergency condition loading.

According to the previous appendices, the version of the FAR23 normative 2012 is used for this design, where the normative determine the calculations of loads in a landing condition. These are:

FAR 23.485 Sideload conditions:

(a) For the side load condition, the airplane is assumed to be level-headed, with only the main wheels contacting the ground and the shock absorbers and tires in their static positions.
(b) The vertical load factor must be 1.33, with only the main wheels contacting the ground and the shock absorbers and tires in their static positions.
(c) The limit side inertia factor must be 0.83, with the side ground reaction divided between the main wheels so that:

(1) 0.5(W) is acting inboard on one side.
(2) 0.33 (W) is acting outboard on the other side.

(d) This condition is assumed to be applied at the ground contact point, and the drag loads may be assumed to be zero.

FAR 23.499 Supplementary conditions for nose wheels.
Assumed that the shock absorbers and wheels are in static positions, the nose gear must accomplish the following conditions:

(a) For aft loads, the limit force components at the axle must be:

(1) A vertical component of 2.25 times the static load on the wheel.
(2) A drag component of 0.8 times the vertical load.

(b) For forwarding loads, the limit force components at the axle must be:
(1) A vertical component of 2.25 times the static load on the wheel.

(2) A forward component of 0.4 times the vertical load.

(c) For side loads, the limit force components at ground contact must be:
(1) A vertical component of 2.25 times the static load on the wheel.
(2) A side component of 0.7 times the vertical load.

(d) For airplanes with a steerable nose wheel controlled by hydraulic or other power, at design takeoff weight with the nose wheel in any steerable position, the application of 1.33 times the maximum static reaction on the nose gear.

(e) For airplanes with a steerable nose wheel with a direct mechanical connection to the rudder pedals, the mechanism must be designed to withstand the steering torque for the maximum pilot forces specified in the normative.

In the design analysis, the numerals d and e are not considered, which is a limitation in the project.

Modeling in CATIA V5 of Landing Gear

According to the established conceptual design, the gear is assembled with the structure of Skiron aircraft. The 3D design is done in the software CATIA V5, shown in Figure 2 for the nose gear and Figure 3 for the main gear.

Figure 2. Design of the nose gear

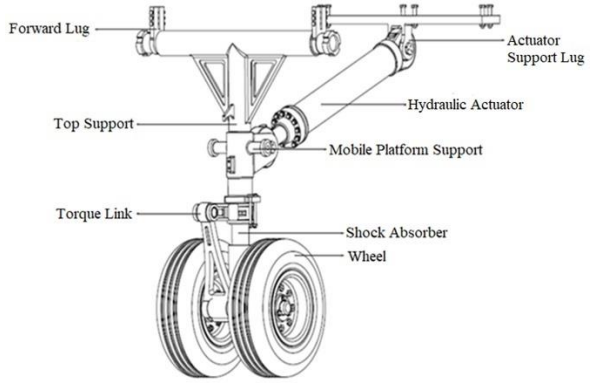

Source: Own source

Figure 3. Design of the main gear

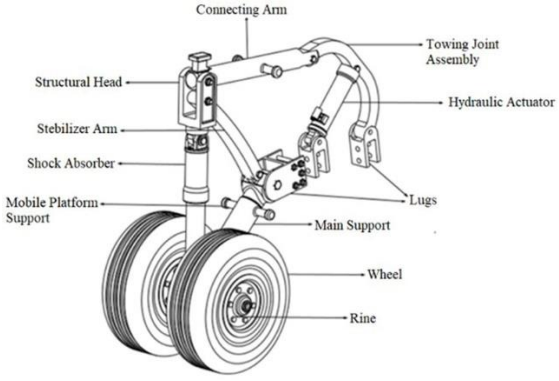

Source: Own source

The 3D design of each gear is the starting point for calculating of the relationship between the parameters and the geometry that must be present in the landing gear in the design stages.

Geometry

According to the engineering development, the geometry of the landing gear is estimated having into account the factors presented in Figure 4.

Figure 4. Geometry parameters of the landing gear

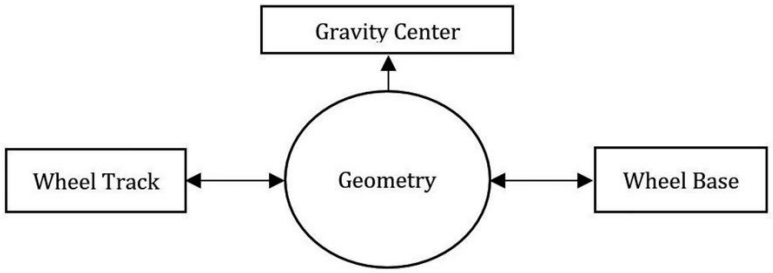

Source: Own source

Calculation of the aircraft's CG

The displacement range of the Longitudinal and Vertical Center of Gravity within the aircraft is identified due to the performance implications contributing to the operation in take-off and landing phases. By variation of the percentage of MAC as in Figure 5 and knowing the geometric dimensions of the aircraft, an estimate is set up for two conditions in operation: the maximum take-off weight (MTOW) and the maximum zero fuel weight (MZFW) [5].

Figure 5. Parameters for CG calculation

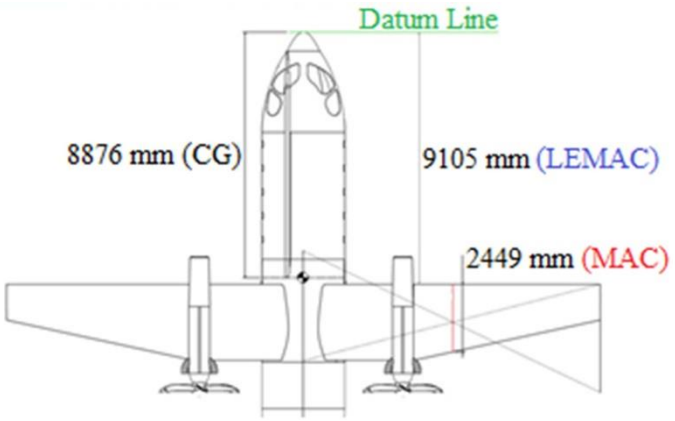

Source: Own source

Through this estimate of the relation between %MAC with the CG in Equation 1, the CG desired will be forward of the main gear according to Equation 2. Consequently, to increase the longitudinal stability regarding the neutral point, it does not enter in stall during the landing and take-off by an induced moment. This condition would need external loads for a stable aircraft.

MAC = 2449 mm
LEMAG = 9105 mm
CG= 8876 mm

$$\%MAC = \left(\frac{CG - LEMAC}{MAC}\right) * 100 = \left(\frac{8876\ \text{mm} - 9105\ \text{mm}}{2449\ \text{mm}}\right) * 100 = -4.401\ \% \quad (1)$$

$$CG_{after}=(0.156*2449\ mm)+8876\ mm=9258.044\ mm$$
$$CG_{forward}=(-0.2444*2449\ \text{mm})+8876\ \text{mm}=8277.4644 mm \quad (2)$$

The delimited area in Figure 6 shows the longitudinal variation of the gravity center within the aircraft.

Figure 6. Graphic weight vs cg (% MAC)

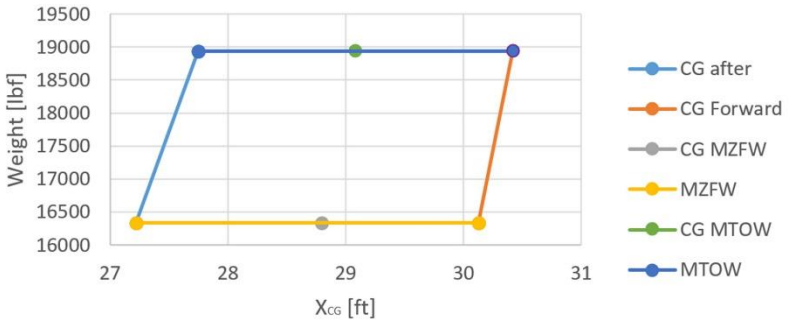

Source: Own source

Vertical CG calculation

The calculation of the vertical CG is obtained by a triangular relationship between the landing gear (shown in the Figure 7) and the aircraft center (shown in the Equation 3).

$$\Delta x = \Delta z\ tan\alpha \quad (3)$$

Figure 7. Simplified diagram of the CG distances in regard to the main gear

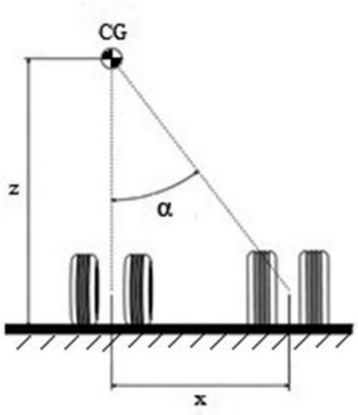

Source: Own source

Estimate x by the Equation 4 and replace x in Equation 5.

$$x = \frac{F_N\, L}{w} = \frac{4227.2546\ N * 6.827\ m}{8618{,}256\ kg\ (9.81 \frac{m}{s^2})} = 0.34135\ m\ \approx 341.35\ mm \tag{4}$$

$$z = \frac{cos\,\alpha}{sen\,\alpha}\ x = \frac{cos\,7.4°}{sen\,7.4°}\ 341.35\ mm = 2628.3\ mm \tag{5}$$

As a result of the estimate, the longitudinal displacement of CG in the aircraft is schematically obtained, as shown in Figure 7.

Figure 7. Center of gravity displacement intervals on the aircraft

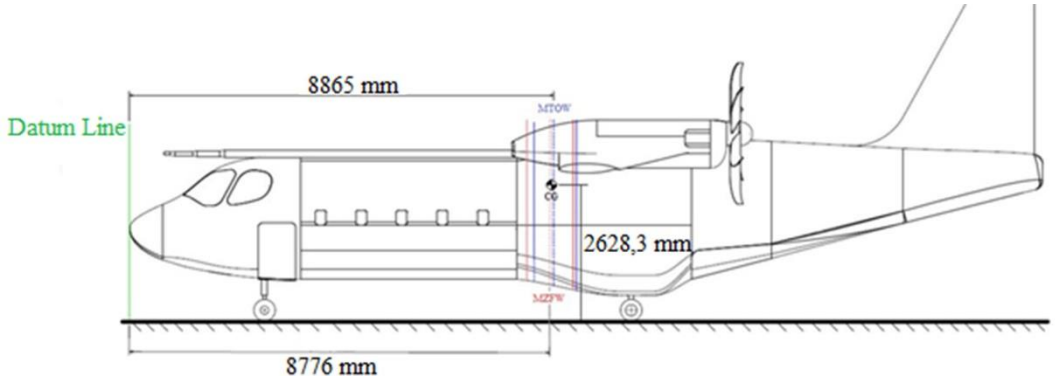

Source: Own source

Wheel Base

The analysis of the wheel base starts with normal reactions on the two landing gears, which are analyzed by a free body diagram, which correlates longitudinal distance between each gear (nose and main gear), according to the Equation 6.

$$F_n = \frac{B_m * W}{B} \; ; \; F_m = \frac{B_n W}{B} \tag{6}$$

Finally, the distance of each one of the gears is describe by Equation 7:

$$B = \frac{B_{m_{max}}}{\%}(\% - 1)$$
$$B_{n_{min}} = B - B_{m_{max}} \tag{7}$$

This distance is obtained according to the displacement of the gravity center in the aircraft for a variation of its weight during operation. The maximum load to support the nose gear is 20%, and the maximum load to support the main gear is 95% [2], getting the next longitudinal distances.

$$B_{m\ min} = 362.102\ mm$$
$$B_{n_{max}} = 6873.621\ mm$$

Given the equality set up in Equation 6 is obtained:

$$F_{n_{max}} = 16910\ N$$
$$F_{m_{max}} = 80322.5\ N$$

Wheel Track

As parameter of empiric design, the trajectory of the wheel must be that the overturn angle would be into the next limit: $\emptyset_{ot} \geq 25°$ [2]. For analysis it is associated with the distribution of the moment generated by two factors that can cause overturning: The centrifugal force in a ground turn and the drag force for cross-wing. The centrifugal force is defined by Equation 8:

$$F_c = m\,\frac{V^2}{R} \tag{8}$$

The analysis of stability and ground control for the aircraft must have the following spacing parameters according to the design associated with the cross-section position length of the two main gears. The space between main gears must be $T > 2Y_{ot}$ [2], T the lateral distance between the two main gears. The turning stability is set by the reaction of two moments: the centrifugal load applied and the aircraft's weight in the Equation 9.

$$Y_{ot} = \frac{F_C * H_{CG}}{W} \tag{9}$$

The result gets for this parameter is:

$$T > 1052.2\ mm$$

Where T = 2357.237 mm in the development of the preliminary design.

For the overturn angle, the Equation 10 is used:

$$\begin{gathered} Y_{ot} = \frac{F_C * H_{CG}}{W} \\ \varphi_{ot} = 26.32° \\ \varphi_{ot} > 25° \end{gathered} \tag{10}$$

Lateral stability by cross-wing force responds to Equation 11, associating the drag aerodynamic force calculation.

$$\begin{gathered} F_w = \frac{1}{2}\rho V_w^2 A_s C_D \\ F_w = 1.264\ N \end{gathered} \tag{11}$$

Finally, the cross-wing force is replaced by the centrifugal force in Y_{ot}, obtaining the same parameter in terms of another variable, shown in Equation 12.

$$Y_{ot} = \frac{F_w * H_{CG}}{W}$$
$$Y_{ot} = 754.38\, mm \tag{12}$$

Where the relation of the following equation is fulfilled ($T > 2\, Y_{ot}$).

Material Selection for Designed Components

The selection and integration of the material in the design follow the methodology that Ashby proposed, presenting a series of four stages applied to a conceptual selection of the material [6]. The development of the methodology is present in Figure 8.

Figure 8. Material selection methodology

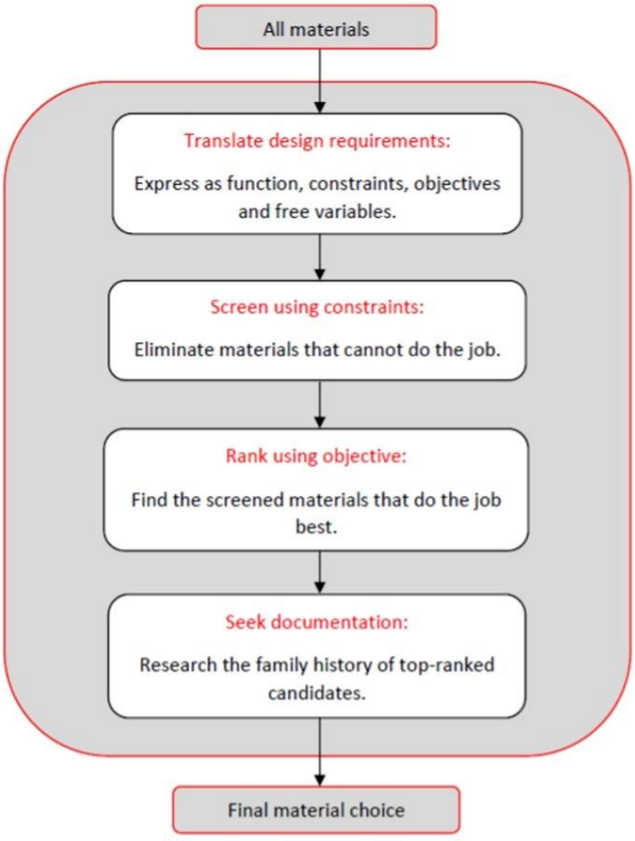

Source: Ashby, Shercliff & Cebon, 2009. [6]

The applications and mechanical properties are obtained from reference to: Articles, the data sheet, and ASM handbook volumes 1 and 2 for aeronautics standards in the science of the material. Material choices are presented in the Table. 1.

According to this, getting the material selection for analysis of each component: The steel AISI/SEA 4340 is used for the Top Support and Main Support, the steel 4130 (Main Lug and Main Actuator Lug), Aluminum 2024-T351 (Forward Lug) and Aluminum 7075-T6 (Actuator Support Lug of Nose), according to the Figure 2 and Figure 3.

Table. 1 Selection materials with their respective properties

Material	Tensile yield strength [MPa]	Ultimate tensile strength [MPa]	Density [g/cm^3]	Modulus of elasticity [GPa]
Aluminum 2024-T351	325	469	2.77	73
Steel 4130	460	560	7.85	190 - 210
Steel AISI/SEA 4340	470	745	7.85	190 - 210
Aluminum 7075-T6	505	570	2.81	72

Source: C. Michael Allen, Metals HandBook VOL 2, 1990. [7]

Analysis of Loads in the Selection Landing Condition

According to Appendix FAR 23.485 [4], the side load conditions are used, as shown in Figure 9.

Figure 9. Reactions in the main gear according to FAR 23

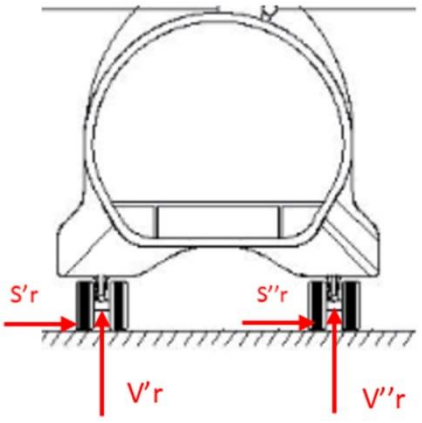

Source: Own source

Where $W = 84516.21\ N$

$$V'_r = V''_r = 56203.28\ \text{N} \qquad S'_r = 42258.11\ N \qquad S''_r = 27890.35\ N$$

Where $V'_r \; and \; V''_r$ is a vertical load factor during the landing condition, S'_r and S''_r is a horizontal load factor applied to the gear, in which the load magnitude changes according to the direction of the application.

The supplementary condition of the nose gear was taken as reference in Appendix FAR 23.499, presented in Figure 10.

Figure 10. Reactions in the nose gear for FAR 23

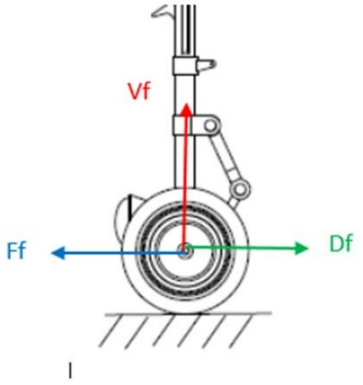

Source: Own source

Where: $V_S = W\frac{b}{d} = 4225.81$ N, in ratio of $^{b}/_{d}$, where $b = B_m$ y $d = B$.

$V_f = 2.25\, V_S$ $= 9508.07\ N$ $\quad$ $D_f = 0.8\, V_f$ $= 7606.46\ N$ $\quad$ $F_f = 0.4\, V_f$ $= 3803.23\ N$ $\quad$ $S_f = 0.7\, V_f$ $= 6655.65\ N$

Combined Load Analysis in the Nose Gear

The analysis of combined loads is performed on the components like Top Support and Main Support. The procedure is started with a free body diagram in the analysis section, which presents the general dimensions of each landing gear (nose and main gear). The simplified scheme of the cross-section analysis is determined in the critical point into the structure, presented in Figure 11, where are applied the combined stress by the loads and resultant moments on each gear [8].

Figure 11. Combined load scheme

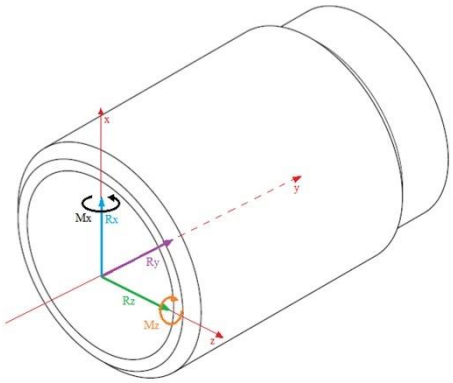

Source: Own source

Applied loads in the analysis point – Nose gear

The reactions in the study point are set by the static analysis of the mechanics, where:

$$R_y = 16903.2421\ N \qquad R_x = 3804.75\ N \qquad R_z = 6658.3125\ N$$

Summary of moments in the cross-section where is the analysis point, due to translation of the forces to the centroid of the section.

$$M_x = 4684.123\ Nm \qquad M_y = 0 \qquad M_z = 2676.642\ Nm$$

Applied loads in the analysis point – Main gear

The reactions on the inclined plane of the study point are set by the static analysis of the mechanics, where:

$$R_y = 59083.6\ N \qquad R_x = -32858.4953\ N \qquad R_z = 0\ N$$

The moments that are acting on the cross-section of the analysis point by the applied forces to the centroid of the section, which are:

$$M_x = 0\ Nm \qquad M_y = 0\ Nm \qquad M_z = -14716.78\ Nm$$

Shear Stress

The shear stress absolute in the analysis point is estimated by the overlay of two loads perpendicular to the axial axis that respond to reactions in X and Z (R_x and R_z), being coplanar to the plane of the analysis section in the component described in the equation 13.

$$\sigma_{yx} = \pm \frac{R_x * Q_1}{I_{zz} * t_1} \pm \frac{R_z * Q_2}{I_{xx} * t_2} \tag{13}$$

Tensors Stress

The tensile analysis of the component is obtained by the reactions and moments applied on the axial axis. There are stresses to direct compression and two bending moments that act perpendicularly to the axial axis for the stress applied to the tensile. Therefore, the absolute tensile stress on landing gear is the overlay of those stress evaluated in the cross-section of the study as is presented in the Equation 14.

$$\sigma_{yy} = \pm \frac{R_y}{A_T} \pm \frac{M_z * C}{I} \pm \frac{M_x * C}{I} \tag{14}$$

Von Mises stress

The estimation is made by the failure theory of the Von Mises criteria to get the Safety Factor at the analysis point [9] by means of Equation 15.

$$\sigma' = \sqrt{{\sigma_1}^2 + {\sigma_2}^2 + {\sigma_3}^2 + 3{\sigma_{yx}}^2} \tag{15}$$

The safety factor of the top support in the analysis point – Nose gear:

$$FS = \frac{470\ MPa}{189.426\ MPa} = 2.481$$

The safety factor of the main support in the analysis point – Main gear:

$$FS = \frac{470\ MPa}{85.2755\ MPa} = 5.51$$

Design and Analysis of Lug in the Landing Gear

This section gives an example of an analysis of the different lugs of the main and nose gear to provide an idea of the failure modes for each lug with the stresses present during the normal operation of the aircraft. Therefore, each lug's shear, bearing, and tensile failure criteria are analyzed according to the applied load [10]. However, the general document in the reference [3] provides all respective procedure for resolving these failure modes.

This analysis uses two different methods for the resolution of the safety factor, which considering appendix FAR 23.2265 and by the design's discretion is stipulated that the safety factor must be greater than 3.5 regarding the ultimate load, without considering factors related to dynamic loads such as fatigue in the normal operation. These methods are: Simplified analysis, which considers an axial load applied to the study lug allows simple assumptions of the nature of the failure [11], and secondly, the method of analysis proposed in "stress Analysis Manual," published by the Air Force Flight Dynamics Laboratory (FDL) in the United States, regarding the Melcon & Hoblit y Bruhn method [12].

Lugs in the nose gear

The nose gear has two different lug designs for the fastening with a bolted joint to the bulkheads of the structure, which correspond to the Forward Lug and Actuator Support Lug of Nose.

Forward Lu

This one has an axial load to the lug, so its respective analysis is simplified. The shape and specific information are shown in Figure 12, which design group proposes. On the other hand, the material selection is aluminum 2024-T351 for calculations and simulations.

Figure 12. Characteristics Forward Lug

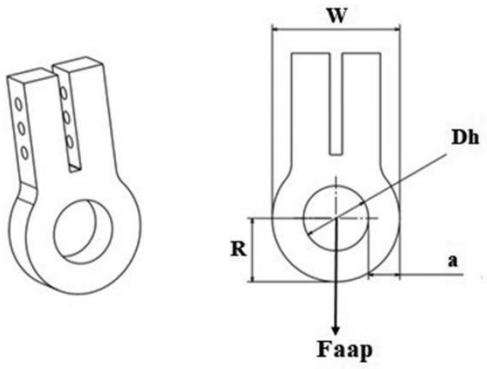

Source: Own source

Where:

F_{app}: 16903.24 N w: 76 mm D_h: 40 mm t = 10 mm R= 38 mm

Depending on the type of load and its respective analysis, the load (F_{app}) and safety factor results for the failure types that can occur are presented below:

- Tensile failure across net section:
  Ultimate tensile load: $P_{tu} = S_{tu} * A_t = 168840\ N$

  Safety Factor: $FS = \frac{P_{tu}}{F_{app}} = \frac{168840\ N}{16903.24\ \text{N}} = 9.988$

- Shear tear out along two planes:
  Ultimate shear load: $P_{su} = S_{su} * A_s = 102600\ N$

Safety Factor: $FS = \frac{P_{su}}{F_{app}} = \frac{102600\ N}{16903.24\ \text{N}} = 6.06$

- Bearing failure:
  Ultimate bearing load: $P_{br} = S_{bru} * A_{br} = 210346\ N$

Safety Factor: $FS = \frac{P_{bru}}{F_{app}} = \frac{210346\ N}{16903.24\ \text{N}} = 12.44$

Lugs in the main gear

The main gear has two different lug designs for fastening with a bolted joint to the bulkheads of the structure with the main gear, which there are three lugs where two have the same geometry as the Main Lug.

Main Lug

The dimensions and characteristics of the main lugs can see in Figure 13, where the proposed material is steel 4130. With this information, the calculations are made according to the proposed method where this lug receives an oblique load [12].

Figure 13. Characteristics of the Main Lug

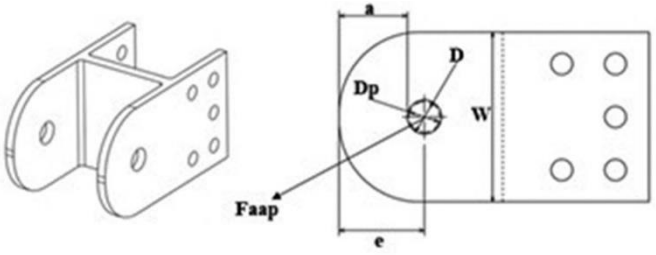

Source: Own source

Where:

D: 26 mm Dp: 25.4mm w: 127 mm e: 63.5 mm F_{app}: 42146.708 N t: 10 mm

According to the oblique load on the landing gear design, the summary of the analysis of this lug is developed, as shown below.

Axial load: Analyzing parameters of geometry and specified material properties (4130 steel). According to the reference method, it is possible to obtain the results in Table 2 for the ultimate design axial load.

Table 2. Parameters results under axial load in the Main Lug

Ultimate Bearing Stress $\boldsymbol{F_{bru.L}} = 1.0864$ GPa	Bushing bearing strength under axial load. (**If there is no bushing in the lug, then the calculation should still be performed assuming that the lug material is the bushing material**). $\boldsymbol{F_{u.B}} = 469.2$ Mpa	Ultimate net-section stress $\boldsymbol{F_{nu.L}} = 468.8$ MPa
Ultimate bearing load $\boldsymbol{P_{bru.L}} = 282.464$ kN	**The bushing ultimate load** $P_{u.B} = \mathbf{155.4065\ kN}$	**Net section ultimate load** $P_{nu.L} = 469.448$ kN

Source: Own source

According to these results, the design ultimate load for an axial load component in the lug is the minimum of the three different loads. So, the axial load component is: $\boldsymbol{P_{u.L.B}} = \mathbf{155,4065\ kN}$.

Transverse load

This analysis is characterized by being like the axial load analysis, considering specific dimensions and getting the following results:

Ultimate transverse load: $P_{tru.L} = 232.96$ kN

Bearing strength for the bushing in a transverse load: $P_{tru.B} = 155.4065$ kN

According to these results, the design load under axial force is identified, corresponding to the minimum value between two types of loads under transverse load. Being this value of: $\boldsymbol{P_{tru.L,B} = 155.4065\ kN}$

Oblique load

The applied load has axial and transverse components, with the loads already calculated previously defining a permissible load curve with Equation 16.

$$\left(\frac{P_{ax.ult}}{P_{u.L,B}}\right)^{1.6} + \left(\frac{P_{tr.ult}}{P_{tru.L,B}}\right)^{1.6} = 1 \tag{16}$$

Where: $P_{ax.ult}$ of Equation 18 *is* the axial component of the final load and $P_{tr.ult}$ is the transverse component of the final load. These two values can calculate using the following relationship of Equation 17.

$$P_{tr.ult} = P_{ax.ult} * tan\,\alpha \tag{17}$$

Where α is the angle of the applied load regarding the axial direction.

$$P_{ax.ult} = \left(\frac{1}{\left(\frac{1}{P_{u.L,B}}\right)^{1.6} + \left(\frac{tan\,\alpha}{P_{tru.L,B}}\right)^{1,6}}\right)^{0.625} \tag{18}$$

Solving the two equations is possible to have the components of the ultimate load with the following values.

$$P_{ax.ult} = \left(\frac{1}{\left(\frac{1}{155.4065\ \text{kN}}\right)^{1,6} + \left(\frac{\tan(29{,}08°)}{155.4065\ \text{kN}}\right)^{1,6}} \right)^{0.625} = 126.435\ \text{kN}$$

$$P_{tr.ult} = 126.435\ \text{kN} * \tan(29{,}08°) = 70.315\ \text{kN}$$

The ultimate applied load is determined by Equation 19.

$$P_{ult} = \sqrt{{P_{ax.ult}}^2 + {P_{tr.ult}}^2} = 144.6722\ kN \quad (19)$$

Finally, the safety factor is calculated according to the last load and the load applied to the lug, showed in the Equation 19.

$$FS = \frac{P_{ult}}{P_{app}} = \frac{144.6722\ kN}{42146.708\ N} = \mathbf{3.432} \quad (20)$$

Finally, the safety factor is calculated according to the last load and the load applied to the lug, showed in Equation 20.

ANSYS Workbench Simulation

The comparison of the theoretical results with the analysis by finite elements was made into the software Ansys Workbench with the Static Structural module for the resistance analysis of the component structures. This was an alternative estimation method to the structural integrity in base on the landing conditions established in the six selected components. The detailed methodology is presented in the reference [3].

The analysis elements are integrated into the structure and mechanism of retraction and extension in Figure 2 and Figure 3 of the Preliminary CAD Modeling of the Landing Gears. The following flowchart establishes the development of simulation protocols in Figure 14.

Figure 14. Simulation Protocol Flowchart

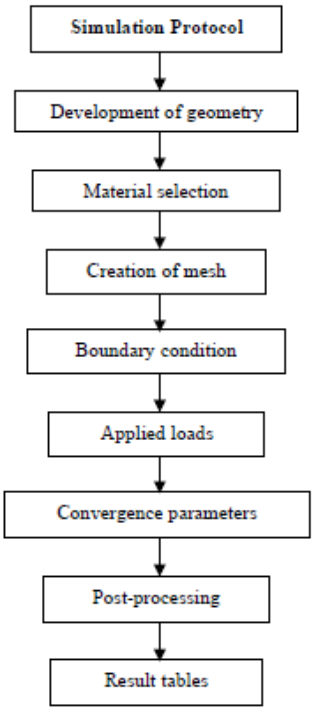

Source: Own source

Creation of mesh

Different types of meshing methods are defined according to geometric characteristics. The components are sectioned according to the type of discontinuity present, such as vertices, curves, and holes, among others. The different types of mesh used are sweep/quadrilateral and pyramidal and hex dominant/quadrilateral. For more complex and bigger components such as top support, the refining of the mesh is made by iterative convergence criterion with the reduction of element size, as shown in Figure 15.

Figure 15. Meshing of the element

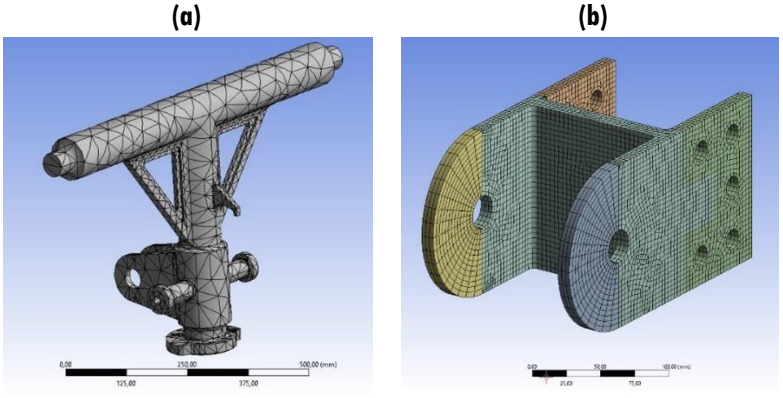

Source: Own source

Boundary conditions: The types of support established by the module of Static Structural of the Ansys Workbench are:

- Fixed: No degree of freedom.
- Cylindrical Support: Only a degree of tangential freedom is applied to cylindrical surfaces.

Applied loads: The structural loads for static analysis into the static structural module of Ansys Workbench are the next: Force and Remote Force.

Results

The variation of the GC range allows obtaining a first approximation of the geometric gear data. Knowing this range is necessary to move the main gear towards the back close to the loader. Since this configuration allows a better performance of the aircraft, placing the GC in front of the main gear avoids an overturn. The aircraft does not require compensation of external loads by operation instability with respect to reference parameters associated with recommended minimum standards for a good operation [2].

The distance percentage (Wheel Base) is expressed in correlation to the percentage corresponding to the weight to be borne by each landing gear. This load percentage changes in proportion to the longitudinal stability criterion of the aircraft associated with the location of CG. The main gear's proximity generated an increase in the contribution to the mechanical stress in the structure of the gear. On the other hand, the wheel track analysis for a condition of lateral stability under the effects of the centrifugal and aerodynamic load. The position of the location of each main gear is validated with the position attached to the fuselage podded.

The safety factor by both methods (Combined Loads and Computational Analysis) is obtained through Von Mises's criteria according to failure theory for the principal stresses. The Von Mises's stress is not exceeding material yield stress for each case, where the element's behavior of the element has been studied in an initial state of stress in which tensile and shear stresses contribute. According to the stress of Von Mises, safety factors regarding the yield stress of the selected material (Steel 4340) are compared with the computational analysis presented in Table 3.

Table 3. FS Results obtained in the theory and simulation for landing gear components

Component	Von Mises Stress	Theory Safety Factor	Ansys Safety Factor	Relative Error
Top Support	189.426 MPa	2.481	2.3	7.3%
Main Support	85.2755 MPa	5.511	4.91	10.91%

Source: Own source

The combination of reactive moments and reactions are loads established in the critical landing condition of the FAA regulation and the longitudinal reaction of the Wheel Base under a static condition, without taking present the effects of failures caused by dynamic loads. The results obtained are compared with the relative error.

The analysis points for each element can be visualized in Figure 16, where the nose gear component (a) and main gear component (b) are represented.

Figure 16. Safety factor in the analysis cross section

(a) (b)

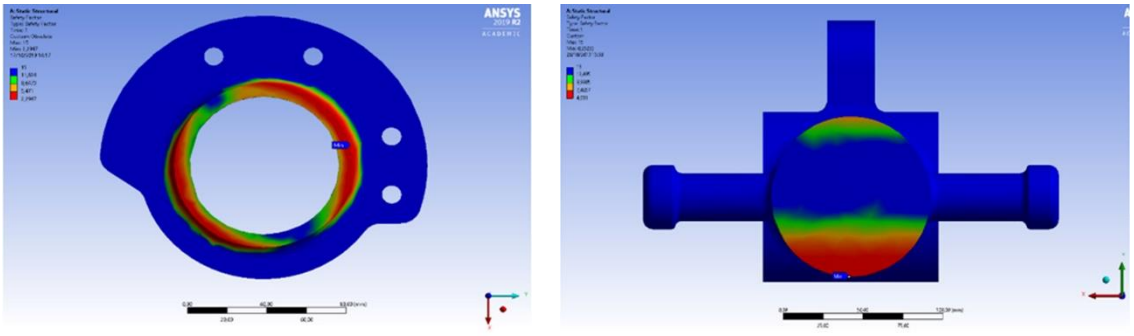

Source: Own source

The design of the lugs about the appropriate geometry and thickness, obtaining a safety factor greater than 3.5, according to the sizing limits set for its manufacture, mechanical attachment, and assembly with other components. Lugs are evaluated in 3 criteria: Bearing, Shear tear failure, and Tensile failure. The results obtained are presented in Table 4, analyzed under the criteria of failure and the direction of force applied in the lug.

To get the safety factor is necessary to calculate the load present in each type of failure together with the properties of the selected material. Using its respective method, the force acts axially (simplified analysis), or an oblique load act on the lug according to the design.

Table 4. Safety Factor for each Lug

Lug	Load	FS
 Forward Lug (Nose Gear)	16903.24 N	Tensile failure FS= 9.988 Shear tear failure FS=6.06 Bearing Failure FS=12.44
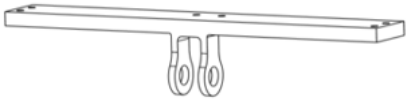 Actuator Support Lug (Nose Gear)	Oblique load 17332.75 N	FS=7.616

Lug	Load	FS
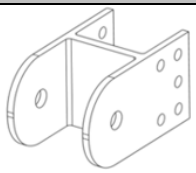 Main Lug (Main Gear)	Oblique load 42146,708 N	FS=3.432
 Actuator Lug (Main Gear)	33715,038 N	Tensile Failure FS= 13.678 Shear Tear Failure FS=4.905 Bearing Failure FS=6.222

Source: Own source

To corroborate the theoretical results by finite elements, the safety factors by shear failure in 4 lugs are used in Figure 17. The comparison of results is presented in Table 5.

Figure 17. Maximum Shear Stress on Lugs

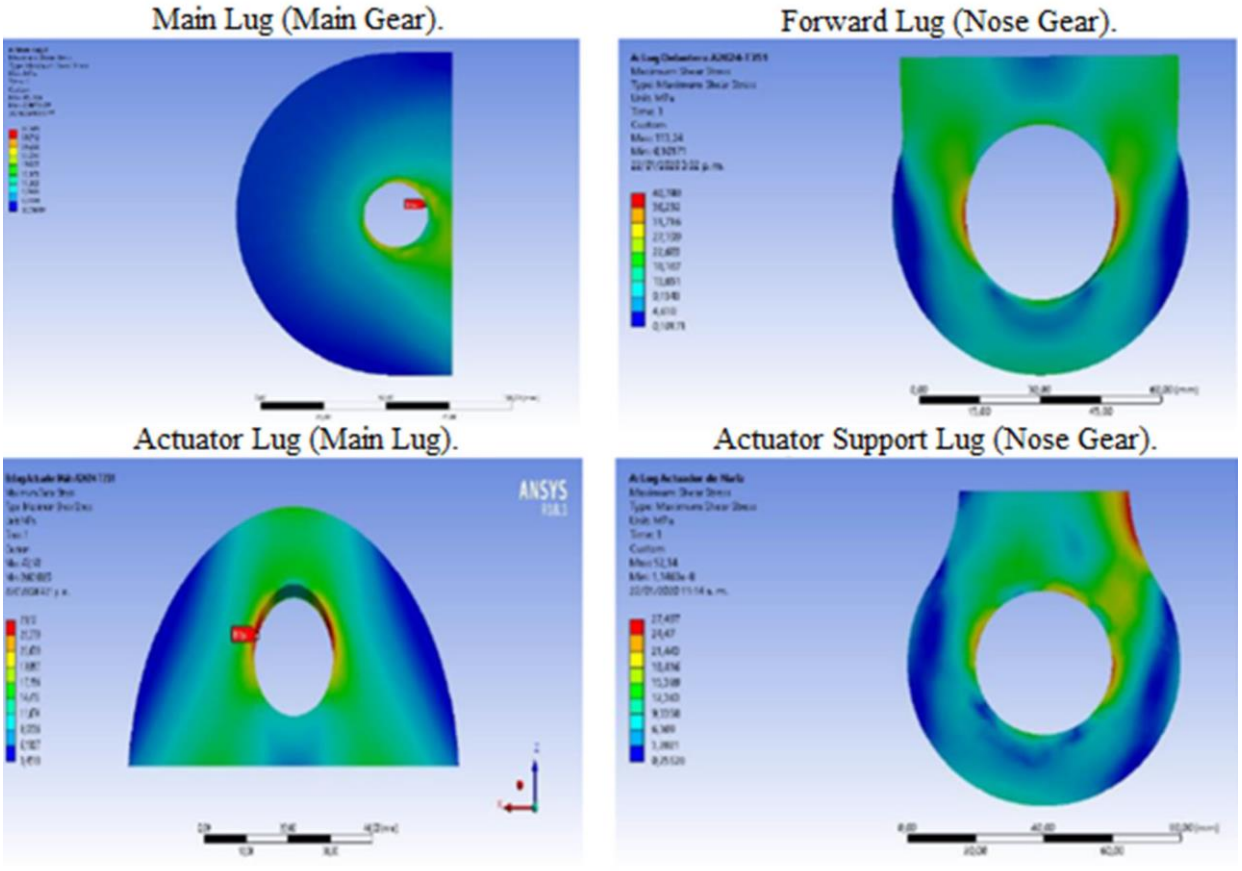

Source: Own source

Table 5. Results of lug in Ansys with their respective Percentage Error

Safety factor	Value by Ansys	Relative error
Forward Lug (Nose Gear)	6.35	4.566%
Actuator Support Lug (Nose Gear)	9.67	20.1%
Main Lug (Main Gear)	4.11	2.968%
Actuator Lug (Main Gear)	4.98	1.6%

Source: Own source

Conclusions

The applied theory emphasizes the geometric development of stability and controllability in the ground on the position of the landing gear. In addition, the volumetric constraints and design requirements are achieved set out for the conceptual model of the aircraft.

The estimation of longitudinal and lateral stability was established in the most critical conditions for the operation of the aircraft, being this with the maximum take-off weight (MTOW), where the main gear is contemplated the critical reaction, it is the 95% of the weight and a 20% in the nose gear.

The development of Finite Element analysis delimited by geometry reactions (Wheel Base) and selected landing conditions assessed the mechanical properties of the selected material against the absorption capacity of the load without presenting permanent deformation into the elasticity limits. We got an operation of the components into the range of the material yield in the presence of induced stress.

Results are obtained from simulations development by Finite Elements, which are acceptable for the regulations of FAA Part 23 with standards associated with the airworthiness, being corroborated with theoretical analysis of combined loads, where are finding errors relative to less than 10%. On the other hand, the safety factors of Shear tear failure in the structural joints (lugs) are determined by computational analysis, being conformed with the theoretical results, ensuring the integrity of the mechanisms to the structure with a safety factor greater than 3.5, relation with sizing criteria of the lug.

References

[1] Departamento Nacional de Planeación, “DNP le apuesta a una política de desarrollo productivo del sector aeronáutico colombiano,” 2017. [Online]. Available: https://www.dnp.gov.co/Paginas/DNP-le-apuesta-a-una-política-de-desarrollo-productivo-del-sector-aeronáutico-colombiano.aspx

[2] M. H. Sadraey, *Aircraft design: a systems engineering approach*, 1ra ed., New Hampshire, USA: John Wiley & Sons, Ltd, 2013.

[3] G. S. Santiago Gonzalez and D. G. Diego Duran, "Diseño preliminar del tren de aterrizaje para una aeronave tipo CESTOL FAR 23," Universidad de San Buenaventura- Bogota, 2020.

[4] Electronic Code of Federal Regulations, "part 23—airworthiness standards: normal category airplanes," 2020. [Online]. Available: https://www.ecfr.gov/cgi-bin/text-idx?SID=c2894c7e493aa181e895875b4dc364c1&mc=true&tpl=/ecfrbrowse/Title14/14cfr23_main_02.tpl

[5] B. G. Shpati, "Aircraft CG Envelopes," p. 40, 2011. https://www.sawe.ca/download/tech2011/Aircraft%20CG%20Envelopes.pdf

[6] M. Ashby, H. Shercliff and D. Cebon, Materials: *Engineering , Science, Processing and Design*. 2009.

[7] C. Michael Allen Adjelian Allen Rubeli Ltd et al., *Metals HandBook, Properties and Selection: Nonferrous Alloys and Special-Purpose Material*, vol. 2, 10th ed. 1990.

[8] L. Pazmany, *Landing gear design for light aircraft*, San Diego: Pazmany Aircraft Corp, 1986.

[9] F. P. Beer, E. R. Johnston, J. T. DeWolf and D. F. Mazurek, Mecánica De Materiales" 5 ed., Mexico: McGraw-Hill, p. 736, 2009.

[10] M. C. Y. Niu, *Airframe Stress Analysis and Sizing*, 2nd ed., 1999.

[11] E. F. Bruhn, *Analysis and Design of Flight Vehicle Structures*, 1973.

[12] G. E. Maddux, L. A. Vorst, J. F. Giessler and T. Moritz, "Stress Analysis Manual," 1969. https://apps.dtic.mil/sti/pdfs/AD0759199.pdf